Ecological Indicators 158 (2024) 111462

Contents lists available at ScienceDirect

Ecological Indicators

journal homepage: www.elsevier.com/locate/ecolind

Original Articles

Global land degradation hotspots based on multiple methods and indicators

Kang Jiang [a,b], Adriaan J. Teuling [c], Xiao Chen [a,b], Na Huang [a,b], Jialin Wang [d], Ziyuan Zhang [e], Riping Gao [a,b], Jingyu Men [a,b], Zhenzhen Zhang [a,b], Yao Wu [a,b], Linlin Cai [a,b], Zhefan Huang [a,b], Zice Ma [f], Zhihua Pan [a,b,*]

[a] *College of Resources and Environmental Sciences, China Agricultural University, Beijing 100193, China*
[b] *CMA-CAU Jointly Laboratory of Agriculture Addressing Climate Change, Beijing 100193, China*
[c] *Hydrology and Quantitative Water Management Group, Wageningen University & Research, Wageningen PO Box 47, 6700 AA, Netherlands*
[d] *Haidian District Meteorological Bureau, Beijing 100088, China*
[e] *Department of Geography, Xinzhou Teachers University, Xinzhou 034000, China*
[f] *School of Geographic Information and Tourism, Chuzhou University, Chuzhou 239099, China*

ARTICLE INFO

Keywords:
Land degradation
Indicators
Field observation
NPP
Vegetation

ABSTRACT

Land degradation is a major impediment to achieving sustainable development. However, there is currently no harmonized global map of land degradation status and hotspots. This paper aims to obtain the status and hotspots map of global land degradation by multiple methods and indicators to give essential references for land degradation neutrality. The results show that there are significant differences in the distribution and degree of land degradation between the different methods and indicators. Validation through observation points reveals that most of the methods and indicators can reflect land degradation in arid and semi-arid areas, while there are suitable methods or indicators in tropical and high-latitude areas. The degree of degradation has a large difference after overlay analysis, which shows that there are shortcomings of different methods and indicators for monitoring the degree of land degradation. However, the overlay of land degradation extent displays a high consistency, reflecting the current state of global land degradation to a certain extent. These areas with high overlay value can be recognized as hotspots of land degradation. It is also found there are consistent water-energy change characteristics in the hotspot area, such as increased land surface temperature and air temperature and decreased soil moisture and precipitation. These results conclude that studies on the degree of land degradation need to be considered in an integrated manner about the regional background. The combination of multiple methods and indicators is recommended for land degradation extent studies in large areas. Comparison of different methods and indicators is important guidance for global land degradation research. Accelerating ecological monitoring and restoration of land degradation hotspots is the first step towards land degradation neutrality.

1. Introduction

The land is essential for human survival as it provides resources such as food, fodder, fuel, and shelter. However, the intensification of human activities and the impacts of climate change have led to significant land degradation, posing a major constraint on human well-being (Lambin et al., 2013). Studies have shown that land degradation negatively affects the living conditions of at least two-fifths of the global population and will reduce global economic output by one-tenth (Willemen et al., 2020). According to Yengoh et al. (2016), approximately 24 % of the global land area was affected by land degradation between 1981 and 2003. As the population grows and climate changes, land degradation becomes more severe. Therefore, managing the relationship between human beings and land and achieving the goal of land degradation neutrality (LDN) are urgent issues to be paid attention.

Land degradation is a complex concept with various definitions. Haigh (2002) defines it as the overall reduction in the productive potential of land, including its major uses such as rain-fed, arable, irrigated, rangeland, and forest, as well as its farming systems and economic value. Warren (2002) thinks land degradation is a very contextual phenomenon and cannot be judged independently of its spatial, temporal, economic, environmental, and cultural context. Therefore,

* Corresponding author.
E-mail address: panzhihua@cau.edu.cn (Z. Pan).

https://doi.org/10.1016/j.ecolind.2023.111462
Received 21 August 2023; Received in revised form 4 December 2023; Accepted 17 December 2023
Available online 23 December 2023

determining land degradation is very difficult. In fact, land degradation is a diverse process that varies in type, scale, and spatial and temporal dimensions. The United Nations Convention to Combat Desertification (UNCCD) defines land degradation as follows: 'The reduction or loss of the biological or economic productivity and complexity of rain fed cropland, irrigated cropland, or range, pasture, forest and woodlands resulting from a combination of pressures, including land use and management practices' and has already been adopted by 197 Parties to the United Nations (Sims et al., 2021; Li et al., 2021). Intergovernmental Panel on Climate Change (Special Report: climate change and land) also aligns with this definition (IPCC, 2019). After reviewing different definitions of land degradation above, vegetation condition, soil condition, biological diversity are the main parts of land degradation's evaluation. The Good Practice Guidance (GPG) provided by UNCCD indicates land degradation by land cover, land productivity and carbon stocks (Sims et al., 2021). In addition, soil physico-chemical properties, Fraction Vegetation Cover (FVC) are also considered as indicators of land degradation. For example, changes in soil composition, such as a decrease in organic matter, can signify soil degradation and impact vegetation and other organisms. Xu et al. (2008) analyzed the frequency of land degradation evaluation indicators in China and globally, based on literature statistics, and found that vegetation cover, slope, organic matter content, land use and land cover, economic level, and biodiversity were the most commonly used indicators in studies.

In addition to the above common indicators of land degradation obtained from the definition of land degradation and literature review, the land degradation assessment method can more comprehensively reflect the land degradation situation. The common methods for assessing land degradation include expert opinions, remote sensing-based methods, land cover change analysis, etc.. The expert opinion method relies on the empirical knowledge of experts and therefore possesses a subjective nature. Currently, although many methods have been developed, the expert opinion method still plays a crucial role because identifying land degradation is inherently subjective and region-specific (Gibbs and Salmon, 2015). With the increasing diversity and accuracy of remote sensing data, remote sensing-based methods have become the mainstream approach for large-area studies (Dubovyk, 2017; Lobell, 2010). This method usually analyzes land degradation with the help of indices such as the Normalized Difference Vegetation Index (NDVI) and Enhanced Vegetation Index (EVI) (Eckert et al., 2015; Gichenje and Godinho, 2018). The land cover change method is one of the most common approaches to land degradation studies. Land cover changes, such as urban and agricultural land expansion, undoubtedly cause soil pollution, soil salinization, and biodiversity loss (Bajocco et al., 2012). Studies have shown that changes in land cover types affect the susceptibility of land to degradation and usually accelerate the process of land degradation (Symeonakis et al., 2007). Furthermore, field observation are commonly employed to validate and optimize the other methods and indicators.

As mentioned above, land degradation process is accompanied by a series of soil and vegetation changes, such as the decrease of FVC and soil organic carbon (SOC), and the deterioration of soil physical and chemical properties. Accordingly, the land surface water-energy conditions in degraded areas will undoubtedly change. From a temperature perspective, land degradation affects changes in soil temperature (Yang et al., 2019). In addition, the land surface temperature (LST) will also increase due to the reduction of surface vegetation cover and the reduction of soil heat capacity (Arribas et al., 2003). From the water perspective, land degradation will directly affect soil moisture, and the reduction of soil evaporation will also affect precipitation (Ibrahim et al., 2015; Seneviratne et al., 2010). Therefore, the changing trend of land surface water-energy conditions after land degradation is also an effective means to verify land degradation.

Due to the differences among various land degradation methods and the complexity of land degradation definition, currently, there is no universally accepted map on the status and extent of global land degradation. However, in the face of intensive human activity and rapid global climate change, there is an urgent need for a concise assessment of global land degradation. Therefore, four land degradation assessment methods (expert opinion, remote sensing-based method, abandoned cropland method, and land use change method) and four indicators (soil organic carbon (SOC), net primary productivity (NPP), biodiversity, and fractional vegetation cover (FVC)) were selected to evaluate global land degradation after summarizing the previous literature. We aim to explore the current global land degradation regions through different methods and indicators and compare different maps from the view of degree and extent by overlay analysis, identify global land degradation hotspots, analyze their water-energy characteristics, and ultimately evaluate the effectiveness of various land degradation methods and indicators using observation data. This research can provide valuable references for governmental decision-making and achieving LDN.

2. Data and methods

2.1. Land degradation methods and indicators

2.1.1. Expert opinion

The expert opinion method is traditional and fundamental in land degradation research. The first world map of human-induced soil degradation was produced by the United Nations Environment Programme (UNEP)-funded Global Assessment of Soil Degradation (GLASOD) project, which was coordinated by the International Soil Reference and Information Centre (ISRIC) in 1990. It is also the only global-scale expert opinion land degradation map that is widely used. The map was compiled with the help of a large number of soil scientists around the world (Gibbs and Salmon, 2015). Therefore, GLASOD map was selected to represent the expert opinion method. The original map includes dominant and subdominant degradation classifications, with each classification comprising four types (chemical deterioration, wind erosion, physical deterioration, and water erosion). Each type is further divided into four degrees (low, medium, high, and very high). The quantification of degradation classifications is as follows: the dominant category accounts for 70 %, and the subdominant category accounts for 30 %. The four types have equal weights, and the three degrees are weighted at 0.33, 0.66, and 0.99 for medium, high, and very high, respectively.

2.1.2. Remote sensing-based method

One of the well-known methods used in global studies is the Global Assessment of Land Degradation and Improvement (GLADA) developed by Bai et al. (2008). This method combines GIMMS NDVI data and MODIS Net Primary Productivity (NPP) data and calculates climate-adjusted NDVI by energy use efficiency. Generally, this method shows a relatively large percentage of degraded land and covers the period from 1981 to 2003. The decreasing trend of the vegetation index is then used to represent land degradation.

2.1.3. Abandoned cropland

Another approach to studying land degradation is the identification of abandoned cropland resulting from declining productivity or ecological and political factors. This method combines expert opinion, agricultural survey data, and remote sensing data to quantify the actual land degradation status rather than estimating potential risk (Gibbs and Salmon, 2015). A recent study by Næss et al. (2021) combined satellite-derived high-resolution land cover maps with an agro-ecological crop yield model to map the global distribution of degraded cropland. This study has a long-time span and high accuracy, making it suitable for our research.

2.1.4. Land cover change

The Global Land Cover (GLC) products released by Global Land Surface Satellite (GLASS) was selected (Liu et al., 2019a) and it is the first record of 34-year-long annual dynamics of global land cover, spanning from 1982 to 2015, at 5 km resolution. It was built with the latest GLASS Climate Data Records (CDRs) and generated on the Google Earth Engine (GEE) platform. The dataset consists of seven land cover classes: cropland, forest, grassland, shrubland, tundra, barren land, and snow/ice. We identified degraded land that were converted to cropland and barren. Transitions from forests to other land types were also considered land degradation.

2.1.5. Soil organic carbon

Soil organic carbon (SOC) refers to the carbon retained in the organic fraction of the soil and is recommended for soil quality testing (Bernoux and Chevallier, 2014; Rajan et al., 2010). Extensive studies have been conducted on the relationship between SOC and land degradation, and it is generally accepted that a decrease in SOC indicates land degradation (Prăvălie, 2021; Prăvălie et al., 2021; Cerretelli et al., 2021; Sainepo et al., 2018). In this study, the global SOC product developed by Zhao et al. (2021) was selected due to its long coverage (1981–2019) and high spatial resolution (5 km). The data were integrated with an improved RothC process model through a spatiotemporal proxy digital soil mapping model, followed by a dynamic simulation of SOC to establish a spatiotemporal sequence reconstruction of SOC. After validation at different regional sample sites around the globe, the R^2 value was found to be 0.406 (Xie et al., 2022).

2.1.6. Net primary productivity

Net primary productivity (NPP) is defined as the amount of organic matter (biomass) remaining in primary producers after cellular respiration (Li et al., 2020a). Numerous research scholars have extensively studied the relationship between NPP and land degradation at regional or global scales (Wessels et al., 2012; Jackson and Prince, 2016; Sutton et al., 2016; Zhang et al., 2020; Zika and Erb, 2009), reaffirming the significance of NPP in understanding land degradation. The data used in this research were obtained from GLASS (https://www.glass.umd.edu/Download.html) and released by the Advanced Very High-Resolution Radiometer (AVHRR).

2.1.7. Biodiversity

A prominent manifestation of land degradation is the decline in biodiversity, making it a widely used indicator in land degradation studies (Gisladottir and Stocking, 2005; Valjavec et al., 2018). For instance, the clearing of vegetation, tillage, grazing, pesticide and herbicide applications, and plantation establishment has been extensively documented as causes of biodiversity decline in agroecosystems (Norton et al., 2013). In this study, the global biodiversity loss map developed by Newbold et al. (2016) was selected due to its new global model based on land pressure and biodiversity, renowned for its high resolution (0.1 degrees) and global continuity (Betts et al., 2017; Johnson et al., 2017; Mace et al., 2018).

2.1.8. Fractional vegetation cover

Fractional vegetation cover (FVC) is a crucial parameter used to describe vegetation degradation, soil erosion, and other factors, often employed in assessing and monitoring land degradation (Chu, 2020; Dashpurev et al., 2023; Liang and Wang, 2020). Many researches have shown that changes in FVC can effectively demonstrate the status and process of land degradation (Dashpurev et al., 2021; Easdale et al., 2019). In this paper, GLASS FVC product based on AVHRR data was selected, which provides a long-term span and high spatial resolution.

2.2. ERA5-Land reanalysis data

ERA5-land reanalysis data were used to analyze the variability of land surface water-energy conditions in degraded areas. The data were provided by the European Centre for Medium-Range Weather Forecasts (ECMWF) and combine ground-based observation and remote sensing data. It is simulated using a new process model, resulting in a comprehensive set of surface water-energy elements (Munoz-Sabater et al., 2021). This reanalysis data set is widely used due to its high temporal and spatial resolution and accuracy (Zou et al., 2022; Zhang et al., 2021). In this study, nine variables were selected: land surface temperature (LST), 2 m air temperature (TEM), precipitation (PRE), soil moisture (SM, 0–7 cm), potential evapotranspiration (EVA), sensible heat flux (H), latent heat flux (LE), net radiation (NR), and atmospheric humidity (AH). The global monthly data from 1981 to 2020 at 0.1-degree resolution were processed as yearly data using MATLAB R2016a (Moler and Little, 2020). In addition, the ratio changes of H or LE account for the sum of energy used to explore energy changes in land-degraded areas.

2.3. MODIS land surface temperature data

MODIS land surface temperature (LST) data were also used to compare multiple datasets to assess LST changes in land degraded areas. Remote sensing data provide higher accuracy and can more realistically reflect LST changes than the reanalysis data. The MOD13A1 product from 2001 to 2020 was downloaded, and it provides global monthly LST at a 0.05° resolution.

2.4. Field observation data

To compare and evaluate the global land degradation maps, a *meta*-analysis was conducted using field observation data from the Web of Science. The keywords used were 'land degradation' and 'field observation'. A total of 499 papers from January 1990 to May 2023 were retrieved, of which 171 were deemed relevant for this study. We extracted the points with latitude, longitude, and degree, finally getting 262 points. The spatial distribution of these points was visualized using ArcGIS 10.2 (Kidd and Liu, 2008) and can be download from Supplementary material.

2.5. Overlay analysis

Overlay analysis was used to explore the differences between the different methods and indicators. First, we resampled different maps to 0.1 degrees and then overlaid the degree and extent of land degradation by ENVI software. The meaning of the overlay value was the number of maps identifying land degradation in each pixel. The degree and extent of different land degradation maps were overlaid separately. The degree of degradation was mainly explored in highly degraded areas (top 20 %) of each map. The overlay of extent of degradation takes all pixels considered degraded.

3. Results

3.1. Spatial distribution of global land degradation under different methods and indicators

Fig. 1 illustrated the spatial distribution of global land degradation obtained by eight different methods and indicators. The degraded areas obtained by different approaches varied greatly. In terms of degraded areas, biodiversity, GLADA and GLASOD accounted for the largest proportion of global land area (except Greenland), 98.5 %, 50.5 % and 33.4 %, respectively. In contrast, the land cover change method, FVC and abandoned cropland method had the smallest area, with only 4.5 %, 14.1 % and 14.1 %, respectively. Regarding the extent of degradation, most of the degraded areas from different methods and indicators were concentrated in the middle and low latitudes. In contrast, in desert regions (e.g., the Sahara Desert) and high latitudes areas, most of the methods and indicators did not show a degradation.

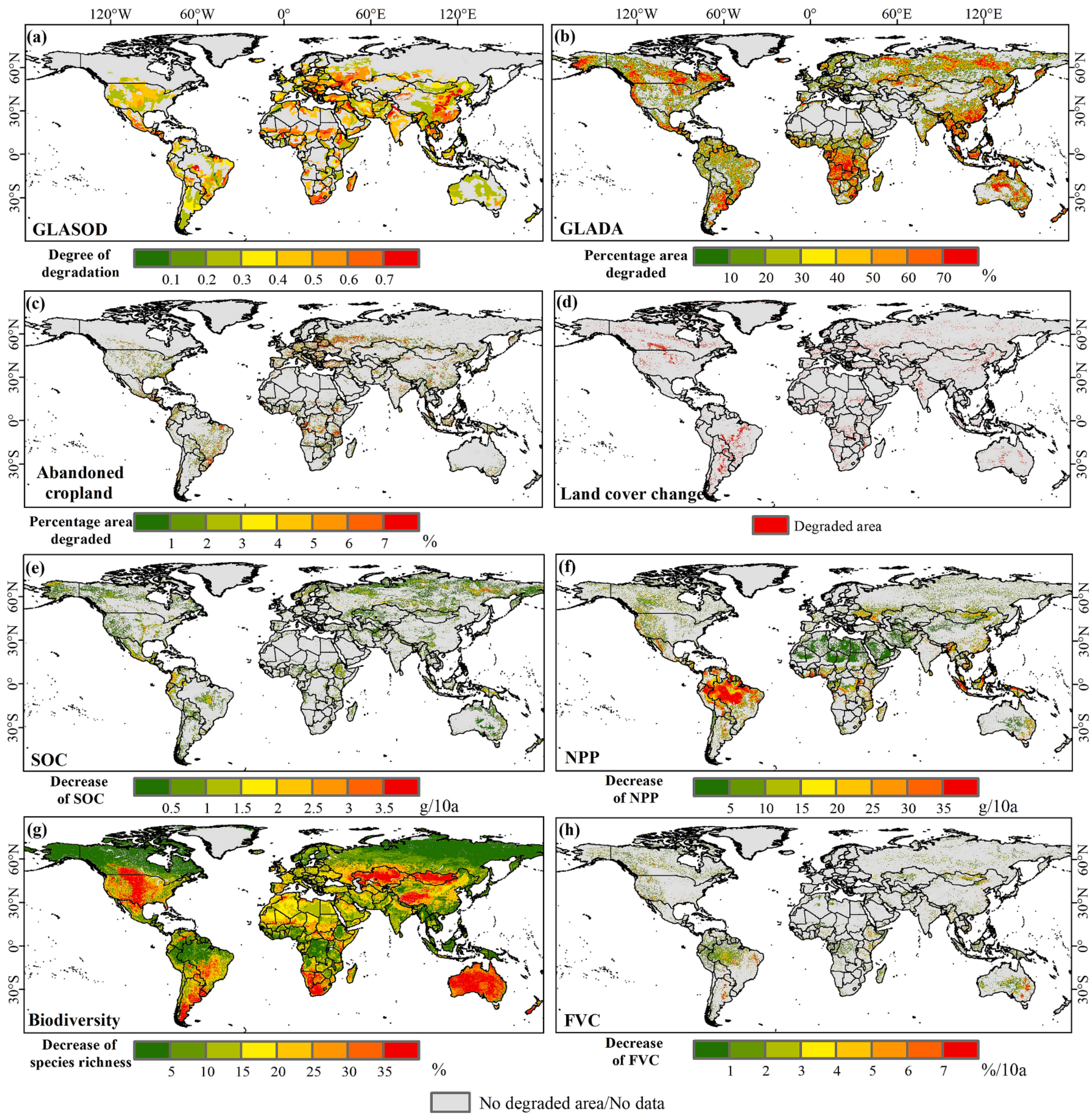

Fig. 1. Distribution of global land degradation based on different methods and indicators. (a) The degree of land degradation after assigning weights according to the type and degree. (b), (c) The proportion of degradation in each pixel. (d) The red color represents the shift of land types judged to be degraded in the direction of degradation. (e), (f), (h) Linear trend of the origin data, with a negative trend representing the degree of degradation. (g) The reduction in species richness. In addition to (d), red represents a high degree of land degradation, and green represents a low degree of land degradation. (For interpretation of the references to color in this figure legend, the reader is referred to the web version of this article.)

3.2. Global land degradation degree by different methods and indicators

In order to compare the degree of eight different maps, the top 20 % degraded areas of 8 maps were overlaid to examine their differences. And the top 20 % degraded areas were considered as highly degraded areas. The map of the top 20 % degraded areas did not exhibit strong consistency, with the highest value was only 6 (Fig. 2). Moreover, areas larger than four accounted for only 1 %. This indicates significant differences in the degree of land degradation by different methods and indicators.

Severely degraded areas obtained by different methods and indicators displayed good agreement in southern North America, central South America, eastern and southern Africa, Central Asia, southern Asia, and eastern Australia, which aligns with the earlier findings. However, there were regions with significant differences, such as the central United States, northern South America, northern Asia, and western Australia.

3.3. The global hotspots of land degradation from the different methods and indicators

In addition to assessing the degree of degradation, understanding the extent of degradation is also crucial. Since the data on biodiversity were worldwide, areas with less than 20 % species declines were excluded. Compared to the degree of land degradation, the extent of land degradation by different methods and indicators exhibited a high consistency (Fig. 3). Areas with high values were mainly distributed in southern and central North America, central South America, eastern Africa, central and southern Asia, and east-central Australia. Nine areas were selected with high land degradation consistency (high overlay values) and defined as land degradation 'hotspots'.

Table 1 provided insights into the trend of land surface water-energy and climatic elements in nine hotspots. The increase in land surface temperature (LST) and 2 m air temperature (TEM), as well as the decrease in precipitation (PRE) and soil moisture (SM), were higher than

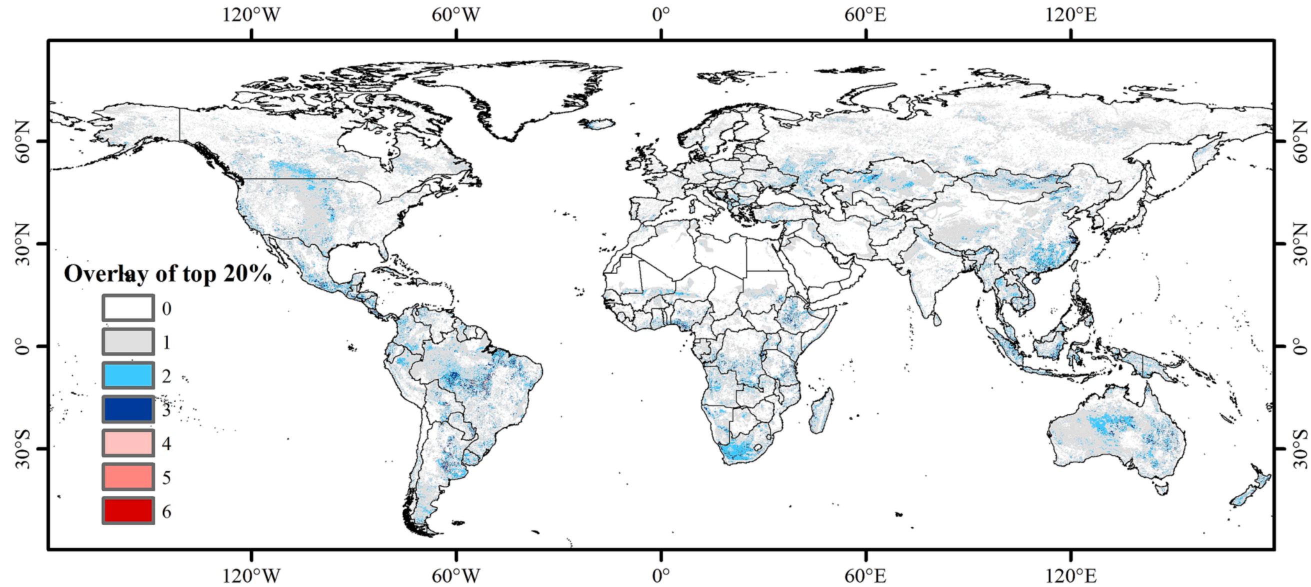

Fig. 2. Overlaid map of the top 20% high degraded areas by different methods and indicators.

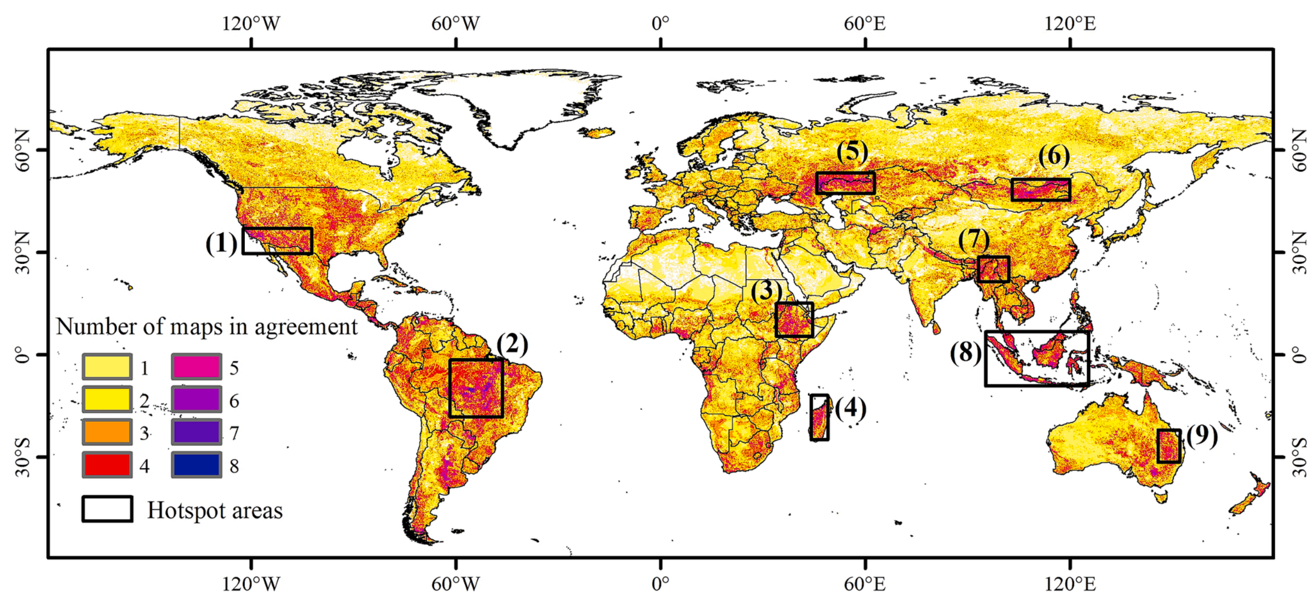

Fig. 3. Global land degradation hotspots from different methods and indicators. Areas with numbers represent areas where a method or indicator indicates land degradation occurrence. The value represents the number of methods or indicators that show the area as degraded.

Table 1
Trends in land surface water-energy and climate elements in 9 hotspots and global mean.

	LST	TEM	PRE	SM	EVA	H	LE	NR	AH
Global mean	0.0302	0.0287	−1.1933	−0.0003	−0.2534	0.0006	−0.0004	1.1464	0.0023
1	0.0504	0.0402	−4.3906	−0.0009	−3.5550	0.0033	−0.0030	−0.9759	−0.0168
2	0.0312	0.0295	−4.4307	−0.0007	−1.5212	0.0012	−0.0012	1.6411	−0.0118
3	0.0327	0.0285	−2.9327	−0.0005	−2.4429	0.0016	−0.0015	−0.9160	−0.0091
4	0.0239	0.0217	−0.3254	−0.0003	−0.7421	0.0006	−0.0005	0.9143	0.0036
5	0.0527	0.0474	−2.5611	−0.0009	−1.7081	0.0038	−0.0038	2.3410	−0.0042
6	0.0507	0.0467	−2.5790	−0.0012	−1.5196	0.0029	−0.0030	1.3391	−0.0036
7	0.0197	0.0189	−12.1143	−0.0003	0.2799	0.0004	−0.0004	2.5769	0.0054
8	0.0119	0.0127	4.6228	0	−0.2010	−0.0004	0.0003	−2.4836	0.0064
9	0.0369	0.0304	−4.1600	−0.0007	−3.5701	0.0025	−0.0017	−1.1578	−0.0025

The full name and unit of water-energy elements are: LST (Land Surface Temperature, °C/a), TEM (Air Temperature, °C/a), PRE (Precipitation, mm/a); SM (Soil Moisture, $m^3/m^3/a$); EVA (Evaporation, mm/a), H (Sensible Heat Flux, %/a); LE (Latent Heat Flux, %/a); NR (Net Radiation, MJ/a); AH (Atmospheric Humidity, g/a).

the global mean state in most hotspots except for (4), (7), and (8). In the areas (5), (6), and (1), the rising trend of LST was significantly higher than global mean (>160 %).

4. Discussion

4.1. Validation of different land degradation methods and indicators based on observation data

In order to validate the accuracy of different methods and indicators, we extract global land degradation field observation points for comparison based on a literature analysis (Fig. 4). It can be observed that the field observation points are primarily concentrated in central Africa and western Asia. And there are fewer observation points in high latitudes. Furthermore, studies on the degree of degradation are relatively limited and primarily distributed in southern Africa.

The accuracy of the different methods and indicators are compared from the continents' view. It is evident that there are fewer observation points in North America, and most of them overlap with different methods and indicators. In South America, most methods and indicators indicate land degradation in this region, particularly in the Amazon region, where degradation is more severe. The NPP and GLADA methods clearly demonstrate degradation, while other methods and indicators either exhibit a lower degree or fail to effectively characterize degradation due to methodological constraints. For instance, in tropical rainforest areas, cropland availability for statistical analysis is limited (abandoned cropland method). Furthermore, despite deforestation and frequent fires, the amount of forest remains huge, making it challenging to capture small-scale deforestation (land cover change method). Regarding Africa, most of the methods and indicators can detect land degradation in the southern Sahara. While in southern Africa, only GLASOD, GLADA, and biodiversity indicators clearly indicate land degradation. In western Asia, only GLASOD, NPP, and biodiversity point to land degradation. The method and indicators align well with the observation sites in central and eastern Asia. In northeastern Australia, GLADA, SOC, NPP, biodiversity, and FVC are consistent with the observations. In addition, most method and indicators fail to reflect land degradation in high-latitude environments. Mainly because the thawing of permafrost leads to increased SM, which promotes vegetation growth. Therefore, vegetation index-related methods and indicators should be cautiously considered in high-latitude regions. Relatively speaking, SOC is a good indicator because microbial activity will increase after the thawing of permafrost. The soil organic matter will be decomposed and release carbon dioxide, thus reducing the SOC content.

We further calculate the number of observation points covered in different maps, and the map area accounts for all global area (Fig. 5). It was evident that the GLADA method covered the highest number of ground observation points (149) and global area (50.5 %). In contrast, the land cover change method covered the fewest ground observation points (10) and global area (4.5 %). When considering the proportion of observation points per unit area, the abandoned cropland method and the SOC indicator exhibited higher proportions. The high proportion observed with the abandoned cropland method can be attributed to the significant expansion and abandonment of farmland, which plays a substantial role in land degradation. As mentioned above, SOC is an important indicator of soil condition and is highly recommended for related studies.

In addition, surface greening is often considered as ecosystem restoration, but it may have negative implications for biodiversity and land conditions. For instance, the complex dynamics behind rangeland greening are influenced by multiple factors (Li et al., 2020b). Potapov et al. (2022) also demonstrate that agricultural activities in South America and Africa, where farmland replaced natural vegetation and tree cover, led to an increase in NPP. Additionally, in degraded sandy areas, the emergence of scrub vegetation may be greener than the original graminoids, potentially misleading remote sensing index methods into identifying it as a vegetation recovery. Therefore, regional studies should combine environmental background analysis and field

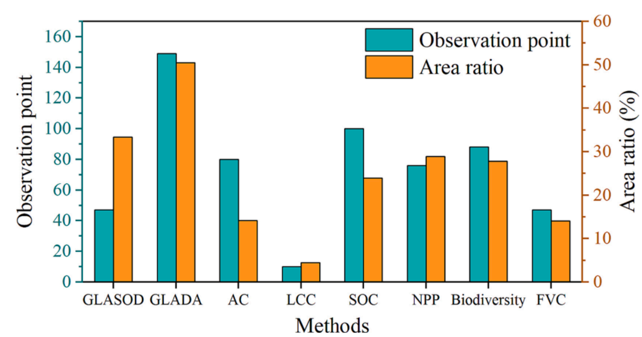

Fig. 5. Statistics of field observation points under the different land degradation and indicators maps and the map area accounts for all global area.

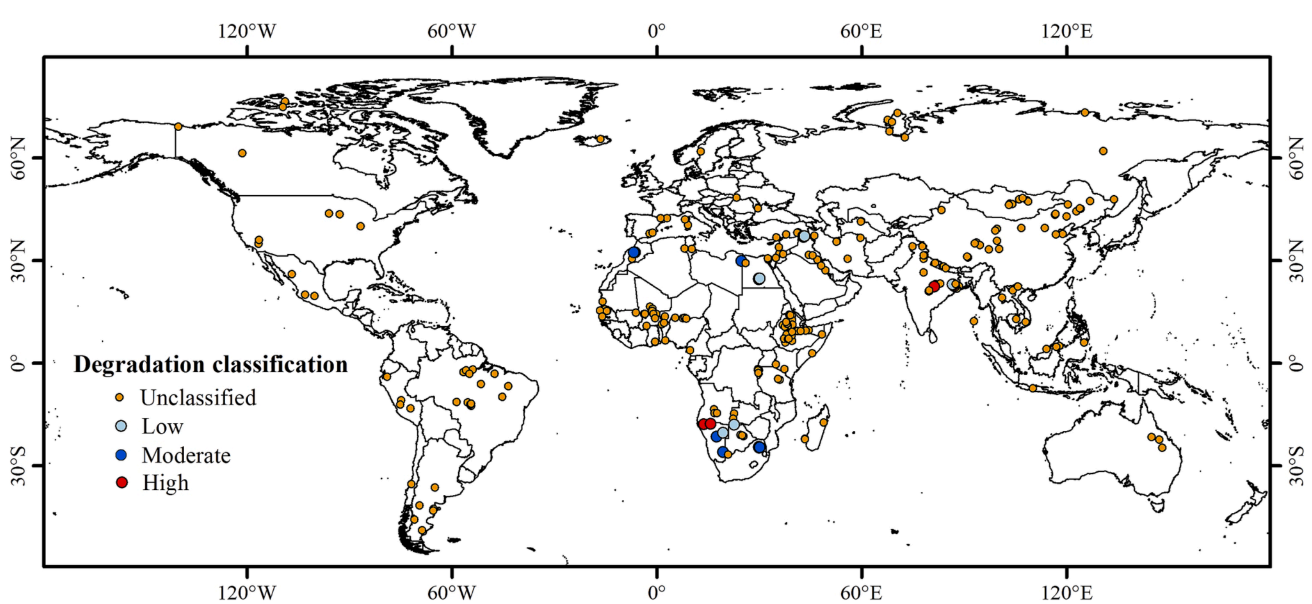

Fig. 4. Spatial distribution of land degradation field observation points.

observation and find the main drivers of land degradation.

The definition of land degradation by different methods and indicators may be incomplete or indicative of only a single element, and therefore the differences in these results are relatively large. For example, GLADA method utilized NDVI and NPP to assess the land degradation status, similar to NPP and FVC indicators. These methods focus on the variation of vegetation, using vegetation growth to reflect the land change rather than the direct condition of the land. Though the abandoned cropland method mainly focuses on cropland, it is an essential reference for global land degradation. Furthermore, the selection of different methods and indicators also has a large impact on the results. Different data sources, start and end of the investigated time frame may show opposite results.

In view of the limitations of the above methodology, we performed an overlay of land degradation results based on the definition of land degradation. Eight methods and indicators also fulfill the UNCCD and IPCC definition of land degradation, i.e. long-term reduction and loss of biological productivity (GLADA, SOC, NPP, FVC), ecological integrity (GLASOD, land cover change, biodiversity), and land values to human (abandoned cropland method). The land degradation evaluation method in the GPG follows 'one out all out' approach, which means that an area can be considered degraded if just one indicator exhibits degradation. This approach is similar to our overlay analysis, in which the degradation performance of each indicator indicates potential degradation in the area. Therefore, we believe that the overlay of these methods and indicators can reflect the current global land degradation status to a certain extent.

4.2. Deficiencies in the identification of the degree of land degradation by different methods and indicators

According to Fig. 2, severely degraded areas obtained by different methods and indicators displayed a good agreement in southern North America, central South America, eastern and southern Africa, Central Asia, southern Asia, and eastern Australia, which aligns with the earlier findings. Previous studies have also highlighted that most of these areas exhibit high levels of degradation. Central North America, sub-Saharan Africa, western Asia, and Australia are characterized by arid and semi-arid climates, which have experienced intensified climate change in recent years, leading to increased occurrences of extreme events such as droughts and high temperatures (Cao et al., 2023; Wang et al., 2014). Studies by Bernardino et al. (2020) have shown shifts and declines in ecosystem functioning in these regions. Climate change and human activities have independently and jointly impacted the ecosystems in these areas. Zika and Erb (2009) have also documented land degradation in these regions. Latin America and Africa have witnessed ecosystem degradation and land degradation in recent decades due to deforestation and agricultural expansion (Foucher et al., 2023; Garcia and Ramos Ballester, 2016; Richards et al., 2014; Zalles et al., 2021). Additionally, southern Asia, including the southern regions of China and Malaysia-Indonesia, also exhibited high values. A study conducted by Li et al. (2016) demonstrates high forest loss rates in these areas. Taken together, the literature suggests that land degradation does occur in areas with high values of high land degradation overlays. All studies suggest that land degradation does occur in areas with high values of land degradation overlays.

In addition, we also conducted a literature review in areas with significant differences such as the central United States, northern South America, northern Asia, and western Australia. First, we analyzed the central region of the U.S.. According to Fig. 1, biodiversity loss was severe in this region. Several studies have reported a significant decrease in bird and ant populations and other species in the region (Fitzpatrick et al., 2011; La Sorte et al., 2017; Peterson, 2003). We found evidence of land degradation and ecosystem degradation in this region through a literature review, primarily attributed to human activities (Bernardino et al., 2020; Li et al., 2016; Liu et al., 2019b; Zika and Erb, 2009). The high intensity of grazing has led to a reduction in Leaf Area Index (Cook and Pau, 2013), NPP (Liu et al., 2019b), and an increased risk of desertification (Huang et al., 2020).

The northern part of South America, including the Amazon region, exhibited a significantly decreasing trend in NPP (Fig. 1f), consistent with the findings of Gang et al. (2022). Moreover, the study carried out by Yu et al. (2022) also shows a significant loss of forest biomass in northern South America. The Amazon region is heavily impacted by human activities, such as the expansion of agricultural lands (Richards et al., 2014; Ross et al., 2017; Zalles et al., 2021) and infrastructure development (Andrade-Núñez and Aide, 2020), as well as deforestation (Bullock and Woodcock, 2021; Li et al., 2016; López, 2022; Walker et al., 2020), which are the main drivers of land degradation. Paredes-Trejo et al. (2022) estimate that 12.67 % of the Amazon basin is degraded, primarily by reduced land productivity, soil organic carbon (SOC) depletion, and land cover degradation. Additionally, fire is a significant disturbance affecting the ecological stability of the region, with frequent occurrence (Wan et al., 2022). Agricultural land, natural grassland, and old-growth forest account for 32 %, 29 %, and 16 % of the annual burned area, respectively (Silveira et al., 2022). Therefore, this area has also undergone a land degradation process.

The highly degraded regions in northern Asia were mainly derived from the GLADA method, while most other methods did not show a significant degraded trend or no data in the region. The high latitude of the region makes it challenging to investigate and less studied. Studies have also indicated a degradation trend in certain grasslands (Liu et al., 2019b) and forests (Li et al., 2016) in the region, influenced by a combination of human and climatic effects. Additionally, an important form of degradation in this region is the permafrost degradation. Studies have shown that permafrost in this region has degraded due to climate change and disturbances (Nitze et al., 2018). The degradation of permafrost leads to changes in soil properties and the conversion of solid water to liquid water in the soil. Sufficient liquid water and warming benefit the growth of vegetation in some permafrost areas, which is the main reason why studies have shown a significant increase in grassland NPP in this region (Liu et al., 2019a).

Western Australia exhibited a severe biodiversity deficit (Fig. 1g). Although there are fewer direct studies on biodiversity change in this region, the literature confirms land degradation in western Australia. Various studies have documented land degradation in this region, ranging from entire ecosystems (Bernardino et al., 2020) to specific habitats such as grasslands (Liu et al., 2019b), forests (Li et al., 2016), and drylands (Zika and Erb, 2009). Human activities predominantly influence land degradation in this region (Bernardino et al., 2020). Additionally, climate change also contributes to the degradation of grasslands in inland areas (Liu et al., 2019b). The degradation of ecosystems inevitably leads to a reduction in biodiversity. Other land degradation methods and indicators did not show high degradation in this area mainly due to its semi-arid climate zone with sparse vegetation. Consequently, the changes in vegetation or SOC are not significant. From the above literature, it can be observed that land degradation has also occurred in most areas with low values of high land degradation overlays.

As a result, we found significant differences and shortcomings in identifying highly degraded areas by different methods and indicators. In studies on the degree of land degradation, it is recommended that an in-depth analysis be carried out with the specific conditions of the area rather than a simple overlay of single or multiple methods and indicators.

4.3. Consistency of land surface water-energy variability in areas with high overlay values

According to Table 1, we can observe that there are significant and consistent changes in land surface water-energy conditions in nine hotspots, such as an increase in LST, TEM, and a decrease in PRE, SM.

This is consistent with the results of other studies, as land degradation generally results in a decrease in SM, vegetation, and soil heat capacity. This leads to an increase in LST and TEM. Reduced SM can also weaken the land–atmosphere water cycle and thus lead to a reduction in PRE (Cuo et al., 2015; Rey et al., 2011; Jiang et al., 2023; Seneviratne et al., 2010; Yang et al., 2019; Arribas et al., 2003).

In addition, we find that the changes in the above elements are not uniform in regions (4), (7), and (8). In the (4) region, the trend of PRE and SM was lower than the global mean, but also displayed a decreasing trend. As SM decreased, H showed an increasing trend while LE decreased. Therefore, both LST and TEM exhibited an increasing trend. The weaker trend in this region may be due to its island background. The large heat capacity of the ocean weakens the warming trend, and water vapor and precipitation from the ocean also weaken the decreasing trends of SM and PRE. In the (7) area, PRE significantly reduced, and the decrease in SM was higher than the global mean. However, the increase in LST and TEM was lower than the global mean. This is mainly because most of the region is covered by forest, and the strong evaporation from the forest mitigates surface warming (Jiang et al., 2022a). Although PRE significantly decreases in the region, it remains at a high level (>2300 mm of 40 years mean), ensuring sufficient water for evaporation and slowing down surface warming (Jiang et al., 2022b). Area (8) exhibited a significant increase in PRE and a decrease in SM, indicating severe land surface water loss. The GLASOD method confirmed water erosion in the area, which negatively affects vegetation. Vegetation index-related methods resulted in a high overlay value for Indonesia. The rising trend of LST and TEM in this region was lower than the global mean mainly due to the high PRE and SM, where more energy reached the atmosphere as LE, leading to a weaker warming trend.

The reanalysis data did not consider land cover for surface hydrothermal impacts, so in order to reduce the bias of the reanalysis data, we also calculated the trends of LST in 9 hotspots using MODIS LST data (Fig. 6). Each hotspot was subdivided into highly degraded areas (overlay value $\geq$ 4) and other areas for comparison. All the mean and median values of LST trends in highly degraded areas were higher than those in undegraded areas. This confirmed our results that the reduced vegetation or decreased SM led to land surface physicochemical properties changes and then accelerated land surface warming. This finding is consistent with other studies that revealed a significant increase in LST in these areas (Liu et al., 2015; Yang and Chen, 2022).

5. Conclusion

This paper identifies and investigates the status and hotspot areas of global land degradation, using various methods and indicators in a comparative perspective. Essentially, the findings obtained in this research can be summarized in several major conclusions.

1. There are significant differences in the extent and degree of land degradation from different methods and indicators. Most methods and indicators can effectively monitor land degradation in semi-arid regions. Vegetation index-related methods and indicators can capture land degradation better in tropical regions. In high-latitude areas, the SOC is a relatively good indicator.
2. The degree of land degradation has a large difference after overlay analysis, while the extent of land degradation exhibits a high consistency. Therefore, it is recommended to consider the regional background and the validation of field observation when studying the degree of land degradation. While when studying the extent of land degradation, it is recommended to overlay multiple methods and indicators.
3. Areas with high overlay values of land degradation extent can be considered hotspots of land degradation. Moreover, most hotspot areas exhibited consistent water-energy variations, such as increased LST and TEM and decreased SM and PRE.

Currently, global land degradation is accelerating, and the comparison of different methods and indicators, as well as the derivation of hotspots, is of great significance for global land degradation research and the implementation of LDN around the world.

CRediT authorship contribution statement

Kang Jiang: Formal analysis, Writing – original draft, Software, Data curation, Conceptualization. **Adriaan J. Teuling:** Writing – review & editing, Supervision. **Xiao Chen:** Writing – review & editing, Software, Methodology. **Na Huang:** Writing – review & editing, Data curation. **Jialin Wang:** Writing – review & editing, Investigation. **Ziyuan Zhang:** Writing – review & editing, Validation. **Riping Gao:** Writing – review & editing. **Jingyu Men:** Writing – review & editing. **Zhenzhen Zhang:** Writing – review & editing. **Yao Wu:** Writing – review & editing. **Linlin Cai:** Writing – review & editing. **Zhefan Huang:** Writing – review & editing. **Zice Ma:** Writing – review & editing. **Zhihua Pan:** Writing – review & editing, Supervision, Conceptualization.

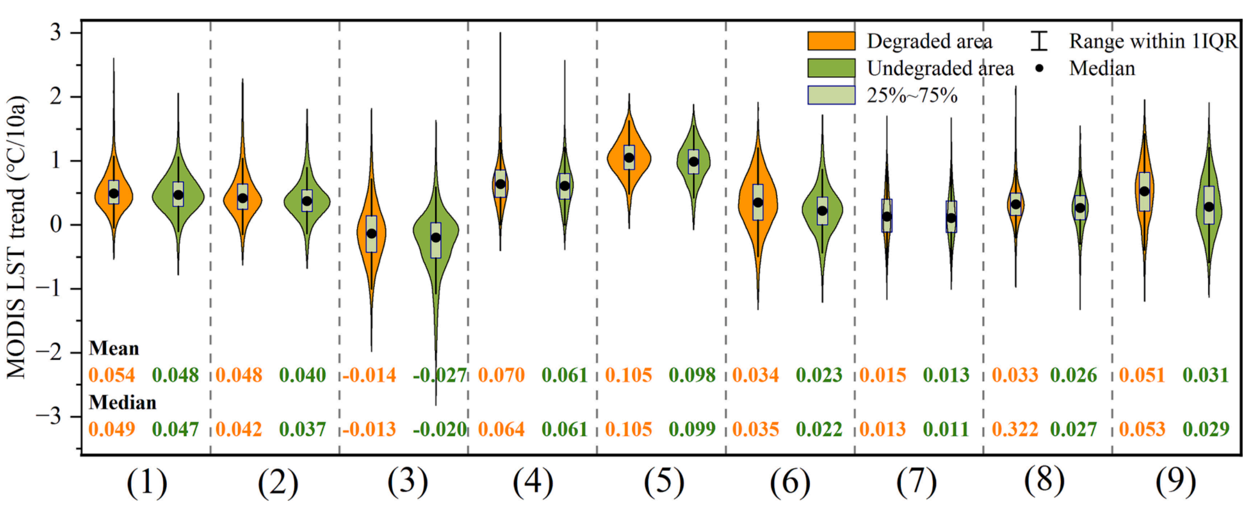

Fig. 6. Comparison of land surface temperature (LST) trends between highly degraded areas in hotspots and other areas. Highly degraded areas are the areas where overlay values $\geq$ 4 of the eight maps. The mean at the bottom of the figure refers to the mean value of all pixels, and the median refers to the median value in all pixels. IQR is an acronym for Inter Quartile Range.

Declaration of competing interest

The authors declare that they have no known competing financial interests or personal relationships that could have appeared to influence the work reported in this paper.

Data availability

Data will be made available on request.

Acknowledgments

This work is supported by the National Natural Science Foundation of China (No. 42271268, 41871086) and Key Research and Development Plan of Inner Mongolia, China (No. 2022YFHH0052)

Appendix A. Supplementary data The spatial distribution of land degradation field observation points from literature review can be downloaded

Supplementary data to this article can be found online at https://doi.org/10.1016/j.ecolind.2023.111462.

References

Andrade-Núñez, M.J., Aide, T.M., 2020. Using nighttime lights to assess infrastructure expansion within and around protected areas in south america. Environmental Research Communications 2.

Arribas, A., Gallardo, C., Gaertner, M.A., Castro, M., 2003. Sensitivity of the iberian peninsula climate to a land degradation. Clim. Dyn. 20, 477–489.

Bai, Z.G., Dent, D.L., Olsson, L., Schaepman, M.E., 2008. Proxy global assessment of land degradation. Soil Use Manage 24, 223–234.

Bajocco, S., De Angelis, A., Perini, L., Ferrara, A., Salvati, L., 2012. The impact of land use/land cover changes on land degradation dynamics: a mediterranean case study. Environ. Manage. 49, 980–989.

Bernardino, P.N., De Keersmaecker, W., Fensholt, R., Verbesselt, J., Somers, B., Horion, S., 2020. Global-scale characterization of turning points in arid and semi-arid ecosystem functioning. Glob. Ecol. Biogeogr. 29, 1230–1245.

Bernoux, M., Chevallier, T., 2014. Carbon in dryland soils—Multiple essential functions, 10th edn, Les dossiers thématiques du CSFD. CSFD/Agropolis International, Montpellier.

Betts, M.G., Wolf, C., Ripple, W.J., Phalan, B., Millers, K.A., Duarte, A., Butchart, S.H.M., Levi, T., 2017. Global forest loss disproportionately erodes biodiversity in intact landscapes. Nature 547, 441-+.

Bullock, E.L., Woodcock, C.E., 2021. Carbon loss and removal due to forest disturbance and regeneration in the Amazon. Sci Total Environ 764.

Cao, C.Y., Guan, X.D., Sun, W., Guo, S.Y., Chen, B., 2023. Changes of extreme high temperature by global warming in the northern hemisphere. J. Appl. Meteorol. Climatol. 62, 3–11.

Cerretelli, S., Poggio, L., Yakob, G., Boke, S., Habte, M., Coull, M., Peressotti, A., Black, H., Gimona, A., 2021. The advantages and limitations of global datasets to assess carbon stocks as proxy for land degradation in an Ethiopian case study. Geoderma 399.

Chu, D., 2020. Aboveground Biomass of Grassland. In: Chu, D. (Ed.), Remote Sensing of Land Use and Land Cover in Mountain Region: A Comprehensive Study at the Central Tibetan Plateau. Springer Singapore, Singapore, pp. 209–227.

Cook, B.I., Pau, S., 2013. A global assessment of long-term greening and browning trends in pasture lands using the GIMMS LAI3g dataset. Remote Sens. (Basel) 5, 2492–2512.

Cuo, L., Zhang, Y.X., Bohn, T.J., Zhao, L., Li, J.L., Liu, Q.M., Zhou, B.R., 2015. Frozen soil degradation and its effects on surface hydrology in the northern Tibetan Plateau. J. Geophys. Res.-Atmos. 120, 8276–8298.

Dashpurev, B., Wesche, K., Jäschke, Y., Oyundelger, K., Phan, T.N., Bendix, J., Lehnert, L.W., 2021. A cost-effective method to monitor vegetation changes in steppes ecosystems: a case study on remote sensing of fire and infrastructure effects in eastern Mongolia. Ecol. Indic. 132, 108331.

Dashpurev, B., Dorj, M., Phan, T.N., Bendix, J., Lehnert, L.W., 2023. Estimating fractional vegetation cover and aboveground biomass for land degradation assessment in eastern Mongolia steppe: combining ground vegetation data and remote sensing. Int. J. Remote Sens. 44, 452–468.

Dubovyk, O., 2017. The role of Remote Sensing in land degradation assessments: opportunities and challenges. European Journal of Remote Sensing 50, 601–613.

Easdale, M.H., Fariña, C., Hara, S., Pérez León, N., Umaña, F., Tittonell, P., Bruzzone, O., 2019. Trend-cycles of vegetation dynamics as a tool for land degradation assessment and monitoring. Ecol. Indic. 107, 105545.

Eckert, S., Husler, F., Liniger, H., Hodel, E., 2015. Trend analysis of MODIS NDVI time series for detecting land degradation and regeneration in Mongolia. J. Arid. Environ. 113, 16–28.

Fitzpatrick, M.C., Sanders, N.J., Ferrier, S., Longino, J.T., Weiser, M.D., Dunn, R., 2011. Forecasting the future of biodiversity: a test of single- and multi-species models for ants in North America. Ecography 34, 836–847.

Foucher, A., Tassano, M., Chaboche, P.-A., Chalar, G., Cabrera, M., Gonzalez, J., Cabral, P., Simon, A.-C., Agelou, M., Ramon, R., Tiecher, T., Evrard, O., 2023. Inexorable land degradation due to agriculture expansion in South American Pampa. Nat Sustain.

Gang, C., Wang, Z., You, Y., Liu, Y., Xu, R., Bian, Z., Pan, N., Gao, X., Chen, M., Zhang, M., 2022. Divergent responses of terrestrial carbon use efficiency to climate variation from 2000 to 2018. Glob. Planet 208.

Garcia, A.S., Ramos Ballester, M.V., 2016. Land cover and land use changes in a Brazilian Cerrado landscape: drivers, processes, and patterns. J. Land Use Sci. 11, 538–559.

Gibbs, H.K., Salmon, J.M., 2015. Mapping the world's degraded lands. Appl. Geogr. 57, 12–21.

Gichenje, H., Godinho, S., 2018. Establishing a land degradation neutrality national baseline through trend analysis of GIMMS NDVI Time-series. Land Degrad. Dev. 29, 2985–2997.

Gisladottir, G., Stocking, M., 2005. Land degradation control and its global environmental benefits. Land Degrad. Dev. 16, 99–112.

Haigh, M.J., 2002. Land use, land cover and soil sciences—land rehabilitation. UNESCO-EOLSS, Oxford.

Huang, J., Zhang, G., Zhang, Y., Guan, X., Wei, Y., Guo, R., 2020. Global desertification vulnerability to climate change and human activities. Land Degrad. Dev. 31, 1380–1391.

Ibrahim, Y.Z., Balzter, H., Kaduk, J., Tucker, C.J., 2015. Land degradation assessment using residual trend analysis of GIMMS NDVI3g, soil moisture and rainfall in sub-saharan West Africa from 1982 to 2012. Remote Sens. (Basel) 7, 5471–5494.

IPCC, 2019. Climate Change and Land: an IPCC special report on climate change, desertification, land degradation, sustainable land management, food security, and greenhouse gas fluxes in terrestrial ecosystems [P.R. Shukla, J. Skea, E. Calvo Buendia, V. Masson-Delmotte, H.O. Portner,¨D. C. Roberts, P. Zhai, R. Slade, S. Connors, R. van Diemen, M. Ferrat, E. Haughey, S. Luz, S. Neogi, M. Pathak, J. Petzold, J. Portugal Pereira, P. Vyas, E. Huntley, K. Kissick, M. Belkacemi, J. Malley, (eds.)].

Jackson, H., Prince, S.D., 2016. Degradation of net primary production in a semiarid rangeland. Biogeosciences 13, 4721–4734.

Jiang, K., Pan, Z.H., Pan, F.F., Wang, J.L., Han, G.L., Song, Y., Zhang, Z.Y., Huang, N., Ma, S.Q., Chen, X., Zhang, Z.Z., Men, J.Y., 2022a. The global spatiotemporal heterogeneity of land surface-air temperature difference and its influencing factors. Sci Total Environ 838.

Jiang, K., Pan, Z.H., Pan, F.F., Wang, J.L., Han, G.L., Song, Y., Zhang, Z.Y., Huang, N., Ma, S.Q., Chen, X., 2022b. Influence patterns of soil moisture change on surface-air temperature difference under different climatic background. Sci Total Environ 822.

Jiang, K., Pan, Z.H., Pan, F.F., Teuling, A.J., Han, G.L., An, P.L., Chen, X., Wang, J.L., Song, Y., Cheng, L., Zhang, Z.Y., Huang, N., Ma, S.Q., Gao, R.P., Zhang, Z.Z., Men, J., Lv, X.Q., Dong, Z.Q., 2023. Combined influence of soil moisture and atmospheric humidity on land surface temperature under different climatic background. Iscience 26.

Johnson, C.N., Balmford, A., Brook, B.W., Buettel, J.C., Galetti, M., Lei, G.C., Wilmshurst, J.M., 2017. Biodiversity losses and conservation responses in the Anthropocene. Science 356, 270–274.

Kidd, D.M., Liu, X.H., 2008. GEOPHYLOBUILDER 1.0: an ARCGIS extension for creating 'geophylogenies'. Mol. Ecol. Resour. 8, 88–91.

La Sorte, F.A., Fink, D., Blancher, P.J., Rodewald, A.D., Ruiz-Gutierrez, V., Rosenberg, K. V., Hochachka, W.M., Verburg, P.H., Kelling, S., 2017. Global change and the distributional dynamics of migratory bird populations wintering in Central America. Glob. Change Biol. 23, 5284–5296.

Lambin, E.F., Gibbs, H.K., Ferreira, L., Grau, R., Mayaux, P., Meyfroidt, P., Morton, D.C., Rudel, T.K., Gasparri, I., Munger, J., 2013. Estimating the world's potentially available cropland using a bottom-up approach. Glob. Environ. Chang. 23, 892–901.

Li, W., Ciais, P., MacBean, N., Peng, S., Defourny, P., Bontemps, S., 2016. Major forest changes and land cover transitions based on plant functional types derived from the ESA CCI Land Cover product. Int. J. Appl. Earth Obs. Geoinf. 47, 30–39.

Li, W., Buitenwerf, R., Chequin, R.N., Florentin, J.E., Salas, R.M., Mata, J.C., Wang, L., Niu, Z., Svenning, J.C., 2020b. Complex causes and consequences of rangeland greening in South America - multiple interacting natural and anthropogenic drivers and simultaneous ecosystem degradation and recovery trends. Geography and Sustainability 1, 304–316.

Li, X.S., Lu, Q., Jia, X.X., 2021. Harnessing big earth data to facilitate land degradation neutrality goals—practices and prospects. Bulletin of Chinese Academy of Sciences 36, 896–903.

Li, F., Meng, J.J., Zhu, L.K., You, N.S., 2020a. Spatial pattern and temporal trend of land degradation in the Heihe River Basin of China using local net primary production scaling. Land Degrad. Dev. 31, 518–530.

Liang, S., Wang, J., 2020. Chapter 12 - Fractional vegetation cover. In: Liang, S., Wang, J. (Eds.), Advanced Remote Sensing (second Edition). Academic Press, pp. 477–510.

Liu, Z.F., Jian, Z.M., Yoshimura, K., Buenning, N.H., Poulsen, C.J., Bowen, G.J., 2015. Recent contrasting winter temperature changes over North America linked to enhanced positive Pacific-North American pattern. Geophys. Res. Lett. 42, 7750–7757.

Liu, Y., Yang, Y., Wang, Q., Khalifa, M., Zhang, Z., Tong, L., Li, J., Shi, A., 2019a. Assessing the dynamics of grassland net primary productivity in response to climate change at the global scale. Chin. Geogr. Sci. 29, 725–740.

Liu, Y., Zhang, Z., Tong, L., Khalifa, M., Wang, Q., Gang, C., Wang, Z., Li, J., Sun, Z., 2019b. Assessing the effects of climate variation and human activities on grassland degradation and restoration across the globe. Ecol Indic 106.

Lobell, D.B., 2010. Remote Sensing of Soil Degradation: Introduction. J. Environ. Qual. 39, 1–4.

López, S., 2022. Deforestation, forest degradation, and land use dynamics in the Northeastern Ecuadorian Amazon. Appl. Geogr. 145.

Mace, G.M., Barrett, M., Burgess, N.D., Cornell, S.E., Freeman, R., Grooten, M., Purvis, A., 2018. Aiming higher to bend the curve of biodiversity loss. Nat. Sustain. 1, 448–451.

Moler, C., Little, J., 2020. A History of MATLAB. Proceedings of the Acm on Programming Languages-Pacmpl 4.

Munoz-Sabater, J., Dutra, E., Agusti-Panareda, A., Albergel, C., Arduini, G., Balsamo, G., Boussetta, S., Choulga, M., Harrigan, S., Hersbach, H., Martens, B., Miralles, D.G., Piles, M., Rodriguez-Fernandez, N.J., Zsoter, E., Buontempo, C., Thepaut, J.N., 2021. ERA5-Land: a state-of-the-art global reanalysis dataset for land applications. Earth Syst Sci Data 13, 4349–4383.

Næss, J.S., Cavalett, O., Cherubini, F., 2021. The land–energy–water nexus of global bioenergy potentials from abandoned cropland. Nat. Sustain. 4, 525–536.

Newbold, T., Hudson, L.N., Arnell, A.P., Contu, S., De Palma, A., Ferrier, S., Hill, S.L.L., Hoskins, A.J., Lysenko, I., Phillips, H.R.P., Burton, V.J., Chng, C.W.T., Emerson, S., Gao, D., Pask-Hale, G., Hutton, J., Jung, M., Sanchez-Ortiz, K., Simmons, B.I., Whitmee, S., Zhang, H., Scharlemann, J.P.W., Purvis, A., 2016. Has land use pushed terrestrial biodiversity beyond the planetary boundary? A Global Assessment. 353, 288–291.

Nitze, I., Grosse, G., Jones, B.M., Romanovsky, V.E., Boike, J., 2018. Remote sensing quantifies widespread abundance of permafrost region disturbances across the Arctic and Subarctic. Nat Commun 9.

Norton, D.A., Reid, N., Young, L., 2013. Ultimate drivers of native biodiversity change in agricultural systems. F1000Research 2, 214.

Paredes-Trejo, F., Barbosa, H., Giovannettone, J., Kumar, T.V.L., Kumar Thakur, M., de Oliveira Buriti, C., 2022. Drought variability and land degradation in the Amazon River basin. Frontiers Earth Sci. 10.

Peterson, A.T., 2003. Projected climate change effects on rocky mountain and great plains birds: generalities of biodiversity consequences. Glob. Change Biol. 9, 647–655.

Potapov, P., Turubanova, S., Hansen, M.C., Tyukavina, A., Zalles, V., Khan, A., Song, X. P., Pickens, A., Shen, Q., Cortez, J., 2022. Global maps of cropland extent and change show accelerated cropland expansion in the twenty-first century. Nature Food 3, 19–28.

Prăvălie, R., 2021. Exploring the multiple land degradation pathways across the planet. Earth Sci. Rev. 220, 103689.

Prăvălie, R., Nita, I.-A., Patriche, C., Niculiță, M., Birsan, M.-V., Roșca, B., Bandoc, G., 2021. Global changes in soil organic carbon and implications for land degradation neutrality and climate stability. Environ. Res. 201, 111580.

Rajan, K., Natarajan, A., Kumar, K.S.A., Badrinath, M.S., Gowda, R.C., 2010. Soil organic carbon - the most reliable indicator for monitoring land degradation by soil erosion. Curr. Sci. 99, 823–827.

Rey, A., Pegoraro, E., Oyonarte, C., Were, A., Escribano, P., Raimundo, J., 2011. Impact of land degradation on soil respiration in a steppe (Stipa tenacissima L.) semi-arid ecosystem in the SE of Spain. Soil Biol. Biochem. 43, 393–403.

Richards, P.D., Walker, R.T., Arima, E.Y., 2014. Spatially complex land change: the indirect effect of Brazil's agricultural sector on land use in Amazonia. Glob. Environ. Chang. 29, 1–9.

Ross, C., Fildes, S., Millington, A.C., 2017. Land-use and land-cover change in the páramo of South-Central Ecuador, 1979-2014. Land 6.

Sainepo, B.M., Gachene, C.K., Karuma, A., 2018. Assessment of soil organic carbon fractions and carbon management index under different land use types in Olesharo Catchment, Narok County, Kenya. Carbon Balance and Management 13.

Seneviratne, S.I., Corti, T., Davin, E.L., Hirschi, M., Jaeger, E.B., Lehner, I., Orlowsky, B., Teuling, A.J., 2010. Investigating soil moisture-climate interactions in a changing climate: a review. Earth Sci. Rev. 99, 125–161.

Silveira, M.V.F., Silva-Junior, C.H.L., Anderson, L.O., Aragão, L.E.O.C., 2022. Amazon fires in the 21st century: The year of 2020 in evidence. Glob. Ecol. Biogeogr. 31, 2026–2040.

Sims, N.C., Newnham, G.J., England, J.R., Guerschman, J., Cox, S.J.D., Roxburgh, S.H., Viscarra Rossel, R.A., Fritz, S., Wheeler, I., 2021. Good Practice Guidance. SDG Indicator 15.3.1, Proportion of Land That Is Degraded Over Total Land Area. Version 2.0. United Nations Convention to Combat Desertification, Bonn, Germany.

Sutton, P.C., Anderson, S.J., Costanza, R., Kubiszewski, I., 2016. The ecological economics of land degradation: impacts on ecosystem service values. Ecol. Econ. 129, 182–192.

Symeonakis, E., Calvo-Cases, A., Arnau-Rosalen, E., 2007. Land use change and land degradation in southeastern mediterranean Spain. Environ. Manage. 40, 80–94.

Valjavec, M.B., Zorn, M., Carni, A., 2018. Human-induced land degradation and biodiversity of Classical Karst landscape: on the example of enclosed karst depressions (dolines). Land Degrad. Dev. 29, 3823–3835.

Walker, W.S., Gorelik, S.R., Baccini, A., Aragon-Osejo, J.L., Josse, C., Meyer, C., Macedo, M.N., Augusto, C., Rios, S., Katan, T., de Souza, A.A., Cuellar, S., Llanos, A., Zager, I., Mirabal, G.D., Solvik, K.K., Farina, M.K., Moutinho, P., Schwartzman, S., 2020. The role of forest conversion, degradation, and disturbance in the carbon dynamics of Amazon indigenous territories and protected areas. Proc. Natl. Acad. Sci. u. s. a. 117, 3015–3025.

Wan, Y., Chen, Y., Li, K., 2022. Identification and spatiotemporal distribution analysis of global biomass burning based on Suomi-NPP VIIRS Nightfire data. J. Clean. Prod. 359, 131959.

Wang, Q.F., Wu, J.J., Lei, T.J., He, B., Wu, Z.T., Liu, M., Mo, X.Y., Geng, G.P., Li, X.H., Zhou, H.K., Liu, D.C., 2014. Temporal-spatial characteristics of severe drought events and their impact on agriculture on a global scale. Quat. Int. 349, 10–21.

Warren, A., 2002. Land degradation is contextual. Land Degrad. Dev. 13, 449–459.

Wessels, K.J., van den Bergh, F., Scholes, R.J., 2012. Limits to detectability of land degradation by trend analysis of vegetation index data. Remote Sens. Environ. 125, 10–22.

Willemen, L., Barger, N.N., ten Brink, B., Cantele, M., Erasmus, B.F.N., Fisher, J.L., Gardner, T., Holland, T.G., Kohler, F., Kotiaho, J.S., von Maltitz, G.P., Nangendo, G., Pandit, R., Parrotta, J.A., Potts, M.D., Prince, S.D., Sankaran, M., Brainich, A., Montanarella, L., Scholes, R., 2020. How to halt the global decline of lands. Nat. Sustain. 3, 164–166.

Xie, E., Zhang, X., Lu, F., Peng, Y., Chen, J., Zhao, Y., 2022. Integration of a process-based model into the digital soil mapping improves the space-time soil organic carbon modelling in intensively human-impacted area. Geoderma 409, 115599.

Xu, N., Guo, X.D., Hong, Y.T., Zhang, C., Hua, D., 2008. Study on Land Degradation Aseessment Indicators based on Literature Analysis. SCIENTIA GEOGRAPHICA SINICA 28, 425–430.

Yang, J.Q., Chen, H.S., 2022. Influences of spring land surface thermal anomalies over west asia on indian early summer monsoon activity and its pathway. J. Clim. 35, 6051–6074.

Yang, W.J., Wang, Y.B., He, C.S., Tan, X.Y., Han, Z.B., 2019. Soil water content and temperature dynamics under grassland degradation: a multi-depth continuous measurement from the agricultural pastoral ecotone in Northwest China. Sustainability 11.

Yengoh, G.T., Dent, D., Olsson, L., Tengberg, A.E., Tucker, C.J., 2016. Development of Land Degradation Assessments. In: Yengoh, G.T., Dent, D., Olsson, L., Tengberg, A. E., Tucker Iii, C.J. (Eds.), Use of the Normalized Difference Vegetation Index (NDVI) to Assess Land Degradation at Multiple Scales: Current Status, Future Trends, and Practical Considerations. Springer International Publishing, Cham, pp. 37–39.

Yu, K., Ciais, P., Seneviratne, S.I., Liu, Z., Chen, H.Y.H., Barichivich, J., Allen, C.D., Yang, H., Huang, Y., Ballantyne, A.P., 2022. Field-based tree mortality constraint reduces estimates of model-projected forest carbon sinks. Nat Commun 13.

Zalles, V., Hansen, M.C., Potapov, P.V., Parker, D., Stehman, S.V., Pickens, A.H., Parente, L.L., Ferreira, L.G., Song, X.-P., Hernandez-Serna, A., Kommareddy, I., 2021. Rapid expansion of human impact on natural land in South America since 1985. Science Advances 7.

Zhang, R.Q., Lu, L., Ye, Z., Huang, F.N., Li, J.D., Wei, L., Mao, T.N., Xiong, Z.L., Wei, S.G., 2021. Assessment of Agricultural Drought Using Soil Water Deficit Index Based on ERA5-Land Soil Moisture Data in Four Southern Provinces of China. Agriculture-Basel 11.

Zhang, Y.Z., Wang, Q., Wang, Z.Q., Yang, Y., Li, J.L., 2020. Impact of human activities and climate change on the grassland dynamics under different regime policies in the Mongolian Plateau. Sci Total Environ. 698.

Zhao, Y., Xie, E., Zhang, X., Peng, Y., 2021. Global topsoil SOC stock from 1981 to 2018 estimated by combining process-based model and space-for-time digital soil mapping (1.0), Zenodo.

Zika, M., Erb, K.-H., 2009. The global loss of net primary production resulting from human-induced soil degradation in drylands. Ecol. Econ. 69, 310–318.

Zou, J., Lu, N., Jiang, H., Qin, J., Yao, L., Xin, Y., Su, F., 2022. Performance of air temperature from ERA5-Land reanalysis in coastal urban agglomeration of Southeast China. Sci Total Environ., 154459